The Journal of Experimental Biology 213, 3187-3197

doi:10.1242/jeb.038760

Spectral and polarization sensitivity of juvenile Atlantic salmon (*Salmo salar*): phylogenetic considerations

C. W. Hawryshyn[1,*], S. D. Ramsden[2], K. M. Betke[2] and S. Sabbah[1]

[1]Department of Biology and Center for Neuroscience Studies, Queen's University, Kingston, Ontario, Canada K7L 3N6 and [2]Department of Biology, University of Victoria, PO Box 3020 STN CSC, Victoria, British Columbia, Canada V8W 3N5

*Author for correspondence (craig.hawryshyn@queensu.ca)

Accepted 2 June 2010

SUMMARY

We were interested in comparing the characteristics of polarization sensitivity in Atlantic salmon to those in Pacific salmon. Here we show that the common ancestor to the clade containing *Salmo salar*, *Oncorhynchus mykiss*, *O. nerka*, *O. clarkii* and *Salvelinus fontinalis* has the trait of ultraviolet polarization sensitivity. We examined spectral and polarization sensitivity of juvenile Atlantic salmon (*Salmo salar*) using both optic nerve compound action potential (CAP) and electroretinogram (ERG) recordings. Our experiments employed photic manipulation to adjust the sensitivity of the four cone mechanisms of Atlantic salmon. A spectrally broad background was used to ensure a contribution of all cone mechanisms to both spectral and polarization sensitivity. Chromatic adaptation was used to isolate the sensitivity of each of the four cone mechanisms for both spectral and polarization sensitivity. Under spectrally broad conditions, UV sensitive (UVS), mid wavelength sensitive (MWS) and long wavelength sensitive (LWS) cone mechanisms contributed to polarization sensitivity. CAP recordings produced the typical 'W' shaped polarization sensitivity curve reflecting two active polarization detectors with peaks at e-vector orientations of 0 deg, 90 deg and 180 deg, and troughs at 30 deg and 150 deg. ERG recordings produced a four-peaked polarization sensitivity curve reflecting two active polarization detectors and negative feedback activity, with peaks at e-vectors 0 deg, 45 deg, 90 deg, 135 deg and 180 deg, and troughs at 30 deg, 60 deg, 120 deg and 150 deg. Polarization-sensitivity measurements of isolated cone mechanisms revealed two orthogonal polarization detector mechanisms in Atlantic salmon, identical to that found in rainbow trout and other Pacific salmonid fishes. Moreover, under spectrally broad background conditions, CAP and ERG polarization sensitivity of Atlantic salmon did not differ significantly from that reported in Pacific salmonids.

Key words: spectral sensitivity, polarization sensitivity, Salmoninae, Atlantic salmon, electroretinogram, compound action potentials, cone photoreceptors, ultraviolet sensitivity.

INTRODUCTION

Polarization sensitivity is a visual attribute of many teleost species (Flamarique and Hawryshyn, 1998; Hawryshyn and McFarland, 1987; Hawryshyn et al., 2003b; Parkyn and Hawryshyn, 2000). Several techniques have been used to describe the mechanisms of ultraviolet (UV) polarization sensitivity such as heart rate conditioning as well as population and single unit recording (Coughlin and Hawryshyn, 1995; Hawryshyn and McFarland, 1987; Parkyn and Hawryshyn, 1993; Parkyn and Hawryshyn, 2000; Ramsden et al., 2008). A salient feature of polarization sensitivity is the presence of differentially sensitive polarization detector mechanisms, which are sensitive to orthogonal e-vector orientations. These detectors, found in many salmonid species, are sensitive to the vertical and horizontal planes of polarization. Functional polarization vision operates in the UV portion of the spectrum only, where the α-band of the UVS cone mechanism mediates the vertical polarization detector, and the β-band of the MWS and LWS cone mechanisms mediates the horizontal polarization detector (Parkyn and Hawryshyn, 1993; Parkyn and Hawryshyn, 2000). Neuronal interaction between the vertical and horizontal polarization detectors, through horizontal cell feedback onto cone photoreceptors, contributes to the coding of e-vector and the ultimate utilization of this information in guiding behavior (Ramsden et al., 2008).

Despite the diverse number of species possessing polarization sensitivity, the use of phylogenetic analysis in understanding the evolution of polarization sensitivity has not been previously studied. Research to date has characterized polarization sensitivity in the genera *Oncorhynchus* and *Salvelinus*, both members of the Salmoninae (Parkyn and Hawryshyn, 2000). When spectral sensitivity and polarization sensitivity were recorded from juveniles of three species of *Oncorhynchus* and one species of *Salvelinus*, four cone mechanisms were evident and polarization sensitivity was found in all species (Parkyn and Hawryshyn, 2000). These results suggest that the UVS cone mechanism is plesiomorphic and that polarization sensitivity may be common to all Salmoninae (Parkyn and Hawryshyn, 2000).

The relationships between the Salmoninae have been constantly revised over the last 50 years (Ramsden et al., 2003), mostly because of the continual change in morphological data sets and the discovery of new synapomorphies. Oakley and Phillips (Oakley and Phillips, 1999) hypothesized, based on molecular evidence, that *Salmo* and *Oncorhynchus* were not sister taxa. Recent reconstruction of the phylogenetic relationships among the Salmonidae, based on more complete mitochondrial and nuclear DNA data sets (Crespi and Fulton, 2004; Ishiguro et al., 2003), however, has revealed that *Salvelinus* and *Oncorhynchus* form sister taxa, with *Salmo* as the outgroup. This new relationship changes past interpretations of trait evolution within the Salmoninae. Therefore, the conclusion that the traits for spectral sensitivity and polarization sensitivity are ancestral to the clade containing *Salmo*, *Oncorhynchus* and *Salvelinus* (Parkyn

and Hawryshyn, 2000) is not sufficient, as *Salmo* has not been characterized electrophysiologically.

In this report, we present the first characterization of spectral sensitivity and polarization sensitivity in the Atlantic salmon (*Salmo salar* L.) using two population recording techniques, compound action potential recordings from the optic nerve (CAP) and electroretinograms (ERG). The similarities between the ERG- and CAP-derived polarization curves from Atlantic salmon and rainbow trout strongly suggest that the peripheral processing of UV polarization sensitivity is conserved between Atlantic and Pacific salmonids.

MATERIALS AND METHODS

Fish care and maintenance

Juvenile Atlantic salmon (*Salmo salar*, 2.45±0.88 g body mass, 8.01±0.69 cm standard length) were obtained from Delrymple hatchery (Stolt Sea Farm Inc., Sayward, British Columbia, Canada). Fish were maintained in tanks continually supplied with fresh water (14±1°C) and held under a 12 h:12 h L:D photoperiod (6500 K fluorescent lamps) in the University of Victoria Aquatic Facility. All experiments were conducted between 09:00 h and 18:00 h to prevent any effects resulting from diel retinomotor movements (Parkyn and Hawryshyn, 2000) or modulation of visual sensitivity through circadian rhythms (Li et al., 2005).

Surgical procedure

Fish were anaesthetized by immersion in a neutrally buffered solution of 125 mg l^{-1} tricaine methanesulphonate (MS-222) until the fish reached stage four anesthesia (Jolly et al., 1972). Subcutaneous injections of a muscle relaxant (pancuronium bromide, 0.05 mg g^{-1} body mass) and a general anesthetic (Maranil, 0.05 mg g^{-1} body mass) were then administered at several sites in the dorsal musculature. The animal was placed in a moistened foam cradle which was held in a Plexiglas® holder, and moistened cheesecloth placed over it to prevent desiccation. A mouthpiece was inserted into the buccal cavity, irrigating the gills continuously with a fresh supply of aerated water (10°C) containing 70 mg l^{-1} MS-222 for anesthesia during surgical manipulation. Ten minutes after the intramuscular injections of anesthetic and paralytic agents, the skin over the right optic tectum was removed using a scalpel, and then the bone over the right optic tectum was removed using a surgical drill with a fine dental burr. The exposed right optic tectum was left intact. The physical condition of the fish was monitored by observing the blood flow through the vascular network serving the brain. The fish was then moved to a restraining cradle in a Faraday cage where the gills were continuously irrigated with aerated fresh water (10°C). Fish were killed by cervical transection at the end of the experiment. All procedures and care of experimental animals were approved by the University of Victoria Animal Care Committee under the auspices of the Canadian Council for Animal Care.

Experimental apparatus

The optical system consisted of two quartz–halogen (250 W, USHIO, Atlanta Light Bulbs, Atlanta, GA, USA) projector lamps for background illumination and a Xenon arc lamp (300 W, USHIO, Atlanta Light Bulbs) for the stimulus channel. Intensity and spectral content of background illumination was manipulated using neutral-density (ND; Inconel on fused silica; Corion, Newport Franklin, Inc., Franklin, MA, USA) and interference cutoff filters (Corion) in the optical path of each background channel. A trifurcated light guide (numerical aperture=0.22, fused silica fibers; Fiberoptic Systems Inc., Simi Valley, CA, USA) provided uniform illumination of the corneal surface of the left eye, combining light from each of the background channels and the stimulus channel. Stimulus wavelength and intensity were controlled by a monochromator (Instruments SA, HORIBA Jobin Yvon Inc., Edison, NJ, USA) and quartz ND wedge (4.0 maximum optical density; CVI Melles-Griot, Rochester, NY, USA). A computer-controlled shutter (Uniblitz, Vincent Associates, Rochester, NY, USA) was used to control the duration of stimuli (square-wave flashes, 500 ms), with flashes being presented approximately 20 s apart, increasing in intensity by 0.2 log units with each step for a total of 2 log units. Spectral sensitivity was measured in 20 nm increments from 360 to 620 nm with wavelength presentation interlaced across the spectrum to prevent chromatic adaptation (Parkyn and Hawryshyn, 2000).

For polarization experiments, a second light pipe (numerical aperture 0.47, Thermo Oriel, Stratford, CT, USA) was used for stimulus delivery. The stimulus was superimposed on the background fields incident on the left eye of the fish. A linear polarizer (HNP'B, Polaroid, Polaroid Corp., Concord, MA USA) was attached to the end of the light pipe, and the e-vector orientation manually adjusted from 0 deg to 180 deg in 30 deg or 15 deg increments. 30 deg e-vector increments were used in CAP recordings, whereas 15 deg e-vector increments were used in ERG recordings. The second light pipe allowed the polarized stimulus to be independent of the background adapting energy, thus removing any adaptation due to polarization. For a given experiment, the stimulus wavelength was chosen to correspond to the λ_{max} of the isolated cone mechanism [UVS cone mechanism λ=380 nm; short wavelength sensitive (SWS) cone mechanism λ=440 nm; MWS cone mechanism λ=540; LWS cone mechanism λ=660 nm]. The background adapting conditions used to isolate the cone mechanisms are specified in Table 1 and the power spectra of these backgrounds is shown in Fig. 1.

Compound action potential and electroretinogram recordings

For this study, we used CAP recording for measuring spectral and polarization sensitivity (Figs 2–7 and Fig. 8B). ERG recording was used for polarization sensitivity only (Fig. 8A).

Compound action potential recording

A sharpened Teflon-coated chlorided silver electrode (0.5 mm diameter, 0.5 mm exposed tip; AM Systems Inc., Carlsborg, WA, USA) was inserted through the right optic tectum rostromedially into the optic nerve of the left eye as described previously (Parkyn and Hawryshyn, 1993; Parkyn and Hawryshyn, 2000). A ground electrode was attached to the caudal peduncle and a chlorided silver reference electrode positioned into the right nares using a

Table 1. Filter combinations and background conditions used in the spectral and polarization sensitivity experiments

Cone mechanism	Isolating chromatic background
Control	700 nm SP, 2.0ND
Ultraviolet-sensitive mechanism (UVS)	500 nm LP, 1.0ND
Short-wavelength sensitive mechanism (SWS)	500 nm LP, 1.0ND + UG-11
Mid-wavelength sensitive mechanism (MWS)	450 nm SP, 1.0ND + 600 nm LP + 1.0ND
Long-wavelength sensitive mechanism (LWS)	550 nm SP

SP, short pass; LP, long pass; ND, neutral density. UG-11 is a broad band filter (Schott) transmitting in the UV range. See Fig. 1 for the power spectra of the background conditions.

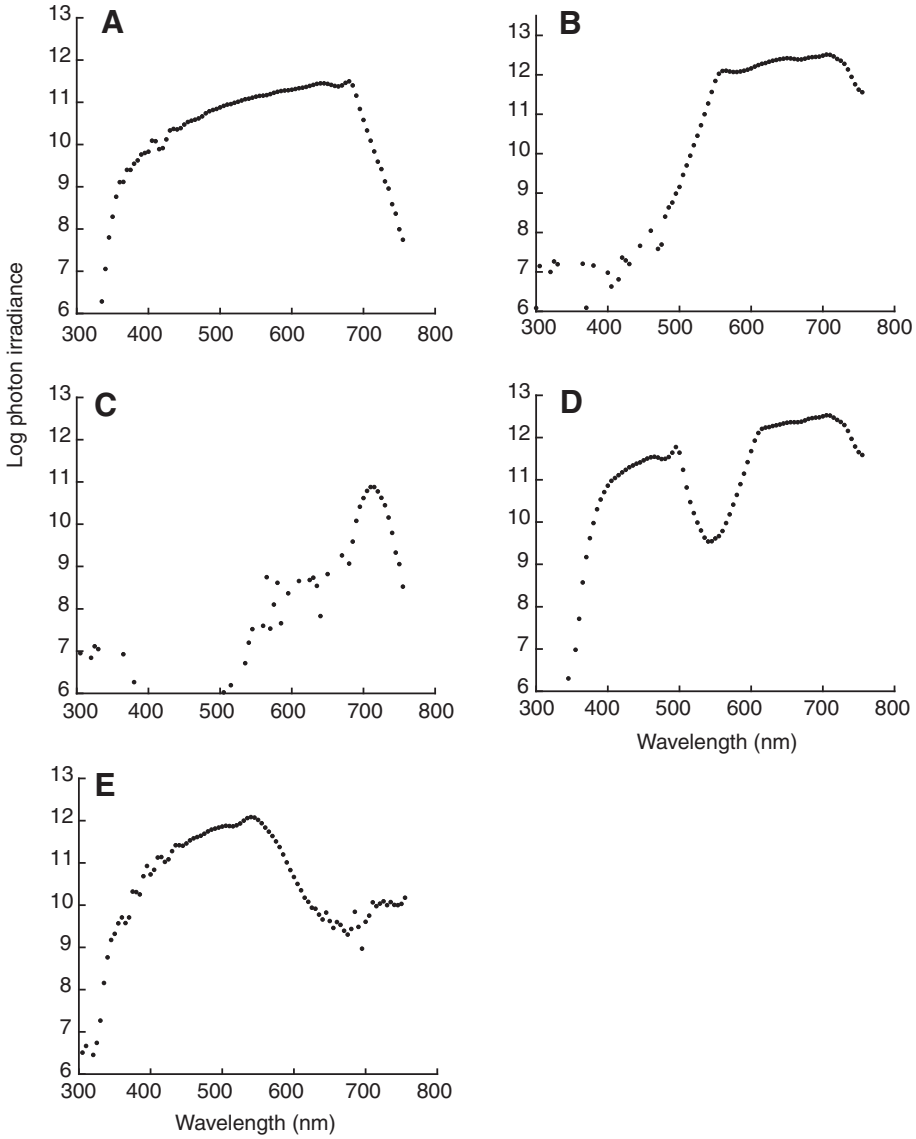

Fig. 1. Log photon irradiance (log photons cm^{-2} s^{-1} nm^{-1}) spectra for background adaptation conditions used in spectral and polarization sensitivity experiments (see Table 1 for filter combinations). (A) Control, broad spectrum background. (B) UVS cone mechanism isolation background. (C) SWS cone mechanism isolation background. (D) MWS cone mechanism isolation background. (E) LWS cone mechanism isolation background.

micromanipulator. The fish was left for 1 h to adapt to the conditions prior to experimentation. Optic nerve responses to light stimulation differ from those recorded from the tectum. As such, physiological comparisons of optic nerve and tectal responses were used to ensure correct trajectory and placement of the electrode. As the electrode penetrated through the tectum, waveform and latency changes indicated the correct depth and trajectory of penetration. For example, latency periods from time of stimulation to time of response were shorter for optic nerve recordings than tectal responses for a particular wavelength. Once the correct depth and trajectory was found, a custom designed stereotaxic apparatus ensured consistent placement of the electrode. Differential recording was used to record optic nerve responses. The recording and reference electrodes and the ground were connected to a Grass Hi-Z probe (Grass-Telefactor, Grass Technologies, West Warwick, RI, USA) and to a Grass Instruments P-5 pre-amplifier (3 Hz low pass filter, 300 Hz high pass filter) with the gain set to 20,000. Signals were then processed with a data acquisition board (National Instruments, Austin, TX, USA).

Electroretinogram recording

A ground electrode was attached to the caudal fin and a chlorided silver reference electrode was positioned with a micromanipulator into the right nares of the fish. A glass electrode [1.5 mm o.d. 1.0 i.d., loaded with saline (0.68 mmol l^{-1})] into a saline-filled half cell (A-M systems, Carlsborg, WA, USA), and the tip positioned using a micromanipulator on the dorsal-nasal surface of the left eye. The fish was left for 1 h to adapt to the conditions prior to experimentation. The stimulus duration was 500 ms with an inter-stimulus interval of 20 s. Differential recording was used to record ERG responses. The recording and reference electrodes and the ground were connected to a Grass Hi-Z probe (Grass-Telefactor, Grass Technologies) and to a Grass Instruments P-5 pre-amplifier (3 Hz low frequency pass filter, 300 Hz high frequency filter, Grass Technologies) with the gain set to 20,000. Signals were then processed with a data acquisition board (National Instruments).

Analysis of optic nerve and electroretinogram responses

For each wavelength or e-vector, the intensity of the stimulus flash was increased in increments of 0.2 ND over a range of 2 ND. The peak amplitude (μV) of both the CAP ON responses and the ERG b-wave at each of these intensities was then plotted against log stimulus irradiance (photons cm^{-2} s^{-1}) to generate a response *versus* intensity (RI) curve. A third order polynomial was fitted to the RI curve. A criterion response value (20 μV) was chosen, which

intersected within the lower linear dynamic range of the RI curve. The intensity required to produce a criterion response was defined as threshold intensity, and sensitivity was in turn defined as the reciprocal of threshold intensity for a given wavelength or e-vector. Spectral sensitivity values were normalized to 440 nm to remove differences in absolute sensitivity between individuals. For polarization experiments, values were normalized between 0 and 1 for each fish. The mean ±1 standard error was calculated for each wavelength or e-vector stimulus condition.

Fitting visual pigment templates

Salmonid fishes have a paired visual pigment system with mixtures of A_1 and A_2 chromophores in both rod and cone outer segments (Temple et al., 2008a; Temple et al., 2008b). To determine the correspondence between visual pigments and sensitivity peaks, only as a first order approximation, absorption templates of visual pigments (Govardovskii et al., 2000) were fitted to the sensitivity curves using a least-squares fit. To generate visual pigment templates we combined absorption spectra for the A_1 and A_2 chromophores as previously described [A_1 derived from equations 1 and 2, and A_2 derived from equations 1 and 6 in Govardovskii et al. (Govardovskii et al., 2000)]. The proportion of the A_2 state was presented using a fraction parameter, a (ranging from 0–1) and therefore, the contribution of A_1 state could be represented as $(1–a)$. Consequently, the absorption spectra of a given cone mechanism exhibiting an A_2 proportion of a was calculated as:

$$A_2(a) = A_1 \cdot (1 - a) + A_2 \cdot a\,. \quad (1)$$

There is a wavelength shift in the λ_{max} of cones over a defined wavelength range as the A_2 proportion changes between 0 and 1 (Harosi, 1994). In salmonids, these ranges correspond to: 370–382 nm (UVS cones), 495–523 nm (MWS cones) and 567–633 nm (LWS cones). Note that there is a negligible spectral shift in the SWS cones so they were not included in this analysis. The λ_{max} shift was also taken into account when generating the visual pigment templates for varying A_2 proportions. Therefore, both the λ_{max} values (Munz and Beatty, 1965; Tsin and Beatty, 1979) and the absorption spectra (Govardovskii et al., 2000) have been used to determine the A_2 proportion of a given cone type. The least-squares fit was performed while leaving the A_2 proportion and a magnitude coefficient unrestricted, allowing Microsoft Excel to find a visual pigment template with an A_2 proportion that best describes the sensitivity peak of concern using a least squares fit. This exercise was performed on the cone isolated under each of the light isolation conditions. Fitting the visual pigment templates to the isolated sensitivity peaks resulted in λ_{max} of 374, 519 and 577 nm corresponding to A_2 proportion of 0.33, 0.85 and 0.15 for the UVS, MWS and LWS cone mechanisms, respectively. The average A_2 proportion that was determined for the various isolated sensitivity peaks was calculated to equal 0.44 and was used for fitting visual pigment templates to the remaining sensitivity peaks obtained under all background isolation conditions. In the case of the SWS cones, a template with an A_2 proportion of 0.44 was fitted to the SWS cone mechanism resulting in a λ_{max} of 432 nm.

Modeling cone contributions

A multiple cone mechanisms model (Coughlin and Hawryshyn, 1994; Hughes et al., 1998; Sperling and Harwerth, 1971) was then used to determine the relative input weight from each cone type to each of the spectral sensitivity curves by assigning weights, which can be positive (excitatory) or negative (inhibitory) for each cone mechanism.

The model takes the general form:

$$S(\lambda) = k_{UVS}\,A_{UVS}(\lambda) + k_{SWS}\,A_{SWS}(\lambda) + k_{MWS}\,A_{MWS}(\lambda) + k_{LWS}\,A_{LWS}(\lambda)\,, \quad (2)$$

where $S(\lambda)$ is sensitivity, $A_{LWS}(\lambda)$, $A_{MWS}(\lambda)$, $A_{SWS}(\lambda)$ and $A_{UVS}(\lambda)$ refer to the spectral absorption coefficients of the LWS-, MWS-, SWS- and UVS-cone visual pigments, respectively, and k_{UVS}, k_{SWS}, k_{MWS}, k_{LWS} are the weight coefficients that represent the contribution of a particular cone mechanism. Fits were performed on restricted parts of the spectrum (bound between the 'notches' in the spectral sensitivity curve) and with different combinations of cone mechanisms. Microsoft Excel was used to perform the least squares fit.

Analysis of polarization sensitivity curves

Normalized polarization sensitivity curves were described by curve fits shown in Eqns 3 and 4:

$$V = m_1 + m_2\,(\cos(m_3\alpha + m_4))^2 \quad (3)$$

$$H = m_1 + m_2\,(\sin(m_3\alpha + m_4))^2\,, \quad (4)$$

where V and H are the response of the vertical and horizontal detector mechanisms, α is the e-vector orientation of the incident light, and m_1–m_4 are curve fit parameters (least squares fit – Kaleidagraph 4.04). A linear subtractive model was used to examine the opponent interactions between the V and H polarization detector mechanisms:

$$S_V = (k_1\,V) - (k_1\,H) \quad (5)$$

$$S_H = (k_3\,H) - (k_4\,V)\,, \quad (6)$$

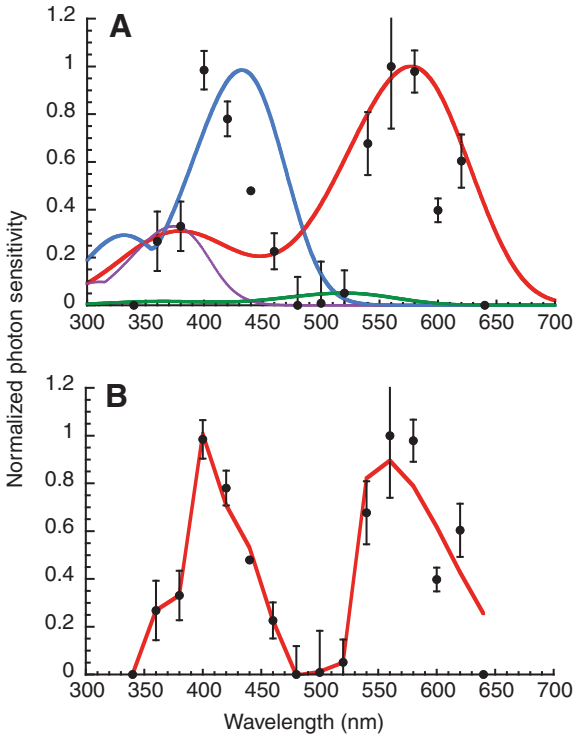

Fig. 2. Mean spectral sensitivity (±1 standard error; N=9) of juvenile Atlantic salmon under white background conditions (filled circles). (A) Least squares fit of visual pigment templates to the mean spectral sensitivity points. UVS cone (violet line), SWS cone (blue line), MWS cone (green line), LWS cone (red line) templates. (B) Least squares fit of the multiple cone mechanism model to the mean spectral sensitivity points (red line). Table 2 lists the curve fitting parameters and R^2.

where, S_v is the sensitivity of the vertical detector mechanism (0–1 on a normalized scale) with the amplitude of inhibitory influence of V and H set by weighting factors k_1 and k_2, and S_H is the sensitivity of the horizontal mechanism (0–1 on a normalized scale) with the amplitude of inhibitory influence of V and H set by weighting k_3 and k_4 (least squares fit – Microsoft Excel).

RESULTS

Spectral sensitivity under white light adaptation conditions

Spectral sensitivity measurements revealed the expression of all cone types under a spectrally broad background (Fig. 2A). Visual pigment templates were fitted to mean sensitivity (Fig. 2A) from 360 to 620 nm. There were discrepancies between the mean spectral sensitivity and the visual pigment templates (λ_{max} values: UVS=374 nm, SWS=432, MWS=519 nm, LWS=577 nm; Table 2), thus opponent interactions were suspected of influencing the spectral sensitivity of the cone mechanisms. We performed a second level of analysis using the multiple cone mechanism model. Fig. 2B shows the model fitted to the spectral sensitivity, which resulted in higher R^2 values (Table 2). Coefficients in Table 2 show opponent interactions occurring where the LWS cone mechanism had an inhibitory influence on the UVS and SWS cone mechanisms at the short wavelength end of the spectrum (k_{LWS}=–7.826). The SWS cone mechanism had a strong inhibitory influence on the MWS and LWS cone mechanisms at the long wavelength end of the spectrum (k_{SWS}=–31.685).

Spectral sensitivity of the UVS cone mechanism

The sensitivity of the UVS cone mechanism was slightly enhanced relative to that of the SWS, MWS and LWS cone mechanisms by chromatic adaptation with a bright yellow background (Fig. 3A). Visual pigment templates (λ_{max} values: UVS=374 nm, SWS=432) were fitted to mean sensitivity (Fig. 3A; Table 2). As the SWS cone mechanism dominated the spectral sensitivity curve under these background conditions it was necessary to further manipulate the sensitivity of the UVS cone mechanism. It is normally quite difficult to isolate the UVS cone mechanism from the SWS cone mechanism because of the high degree of spectral overlap in sensitivity. To confirm an independent UVS cone mechanism, it was necessary to perform UV chromatic adaptation and calculate a difference curve (Fig. 3B). The difference spectrum was then fitted with the UVS cone visual pigment template. The correspondence of the difference curve and the absorbance template (R^2=0.848; Table 2) verified the identity of a UVS cone mechanism.

Table 2. Coefficients and R^2 values for visual pigment templates and multiple cone mechanisms fit to spectral sensitivity curves

Part A. Template fitting

		Fit properties			
	Cone mechanism	UV	SWS	MWS	LWS
	λ_{max}	374	432	519	577
Background condition	A2 proportion	0.44	0.44	0.44	0.44
White spectrally broad (Fig. 2A)	Fit spectral range	360–380	380–480	480–520	560–620
	R^2	0.722	0.167	0.983	0.783
UV cone mechanism isolation (Fig. 3A)	Fit spectral range	360–380	380–480		
	R^2	0.628	0.570		
UV cone mechanism isolation	Fit spectral range	360–380			
Difference curve (Fig. 3B)	R^2	0.848			
SWS cone mechanism isolation (Fig. 4A)	Fit spectral range	360–380	380–480	520–540	560–620
	R^2	1.000	0.970	0.896	0.279
MWS cone mechanism isolation (Fig. 5A)	Fit spectral range	360–420	420–440	460–540	560–620
	R^2	0.853	0.999	0.905	0.539
LWS cone mechanism isolation (Fig. 6A)	Fit spectral range	360–380	420–480	460–520	560–620
	R^2	0.998	0.651	0.219	0.923

Part B. Model fitting

Background condition	Fit spectral range	UVS	SWS	MWS	LWS	R^2
White spectrally broad (Fig. 2B)	340–380	8.071	0.287		–7.826	1.000
	400–460	4.267	0.972		–2.337	0.979
	480–520			–1.910	0.244	0.986
	520–640		–31.685	10.616	0.597	0.783
SWS cone mechanism isolation (Fig. 4B)	340–380	1.198	–0.608			0.473
	400–500	0.130	1.064			0.970
	520–580		–4.497	1.893	–0.394	0.981
	580–640			–2.065	0.615	0.178
MWS cone mechanism isolation (Fig. 5B)	340–400	4.055	0.178			0.798
	400–440	–1.226	1.207			0.940
	460–540			1.059	–0.364	0.717
	360–540			1.219	–0.814	0.858
	560–600			0.969	–0.121	0.575
LWS cone mechanism isolation (Fig. 6B)	360–620			–0.286	0.937	0.821

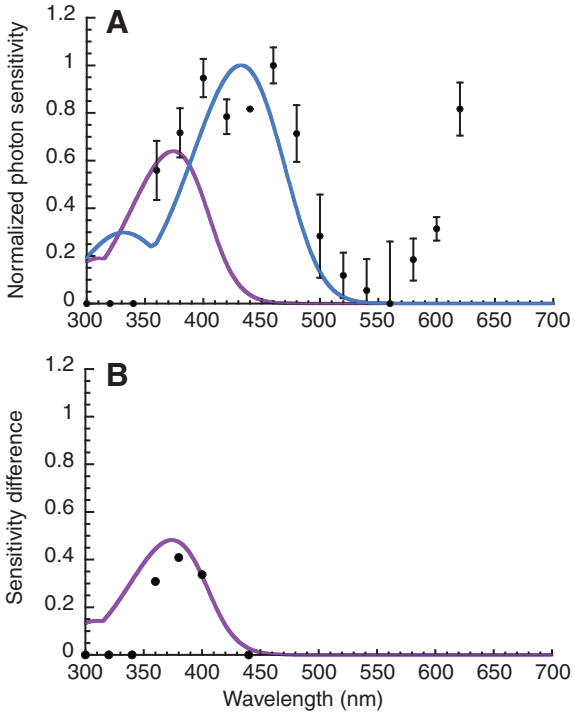

Fig. 3. Mean spectral sensitivity (±1 standard error; *N*=8) of juvenile Atlantic salmon under UVS cone mechanism isolation conditions (filled circles). (A) Least squares fit of visual pigment templates to the mean spectral sensitivity points. UVS cone (violet line), SWS cone (blue line) templates. (B) Difference spectrum (*N*=1) resulting from UVS cone mechanism light adaptation with the addition of a UV background. UVS cone (violet line) template. Table 2 lists the curve fitting parameters and R^2.

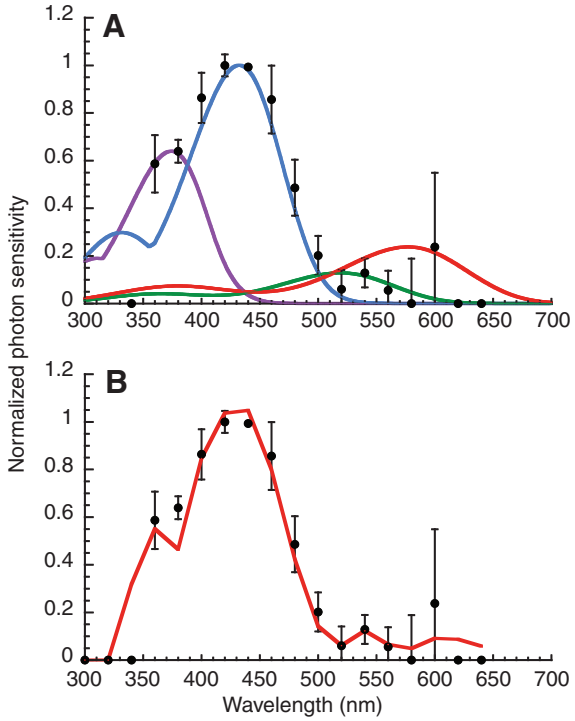

Fig. 4. Mean spectral sensitivity (±1 standard error; *N*=8) of juvenile Atlantic salmon under SWS cone mechanism isolation conditions (filled circles). (A) Least squares fit of visual pigment templates to the mean spectral sensitivity points. UVS cone (violet line), SWS cone (blue line), MWS cone (green line), LWS cone (red line) templates. (B) Least squares fit of the multiple cone mechanism model to the mean spectral sensitivity points (red line). Table 2 lists the curve fitting parameters and R^2.

Spectral sensitivity of the SWS cone mechanism

The sensitivity of the SWS cone mechanism was enhanced using a bright yellow background and a UG-11 filter with high transmission in the UV part of the spectrum (Fig. 4A). Visual pigment templates (λ_{max} values: UVS=374 nm, SWS=432, MWS=519 nm, LWS=577 nm) were fitted to mean sensitivity (Fig. 4A; Table 2). The multiple cone mechanism model improved the fit (Fig. 4B; Table 2). There were opponent interactions (Table 2), but given the degree of isolation of the SWS cone mechanism, these opponent interactions were moderate in scale (k_{SWS}=–4.497 and k_{MWS}=–2.065).

Spectral sensitivity of the MWS cone mechanism

The MWS cone mechanism sensitivity was isolated using long wavelength and short wavelength background conditions (Fig. 5A). Visual pigment templates (λ_{max} values: UVS=374 nm, SWS=432, MWS=519 nm, LWS=577 nm) were fitted to the mean sensitivity (Fig. 5A; Table 2). There were discrepancies between the templates and the sensitivity points evident in the mid to long wavelength portion of the spectral sensitivity curve, which were possibly due to opponent interactions. Fig. 5B shows the multiple mechanism model fit and the coefficients in Table 2 indicate a minor opponency between the MWS and LWS cone mechanisms in the mid to long wavelength part of the spectrum (k_{MWS}=0.969 and k_{LWS}=–0.121).

Spectral sensitivity of the LWS cone mechanism

The sensitivity of the LWS cone mechanism was isolated using short and mid-wavelength background conditions (Fig. 6A). The LWS visual pigment template was fitted to the mean sensitivity (Fig. 6A; Table 2). Fig. 6B shows the multiple cone mechanism model fit and the coefficients in Table 2 indicate a minor opponency between the MWS and LWS cone mechanisms in the mid to long wavelength part of the spectrum (k_{MWS}=–0.286 and k_{LWS}=0.937).

Polarization sensitivity of isolated cone mechanisms

Polarization sensitivity measurements made on isolated cone mechanisms resulted in unimodal curves of vertical and horizontal polarization sensitivity (Fig. 7, see Table 3 for curve fit parameters and R^2 values). When the UVS cone mechanism was isolated, the highest sensitivity was at the vertical e-vector orientation (0 deg and 180 deg; Fig. 7A). However, when the UVS cone mechanism was light adapted with a UV background, UVS cone mechanism polarization sensitivity disappeared (Fig. 7E). Like other salmonid and cyprinid species investigated thus far (Hawryshyn and McFarland, 1987; Parkyn and Hawryshyn, 2000), the SWS cone mechanism did not show significant depth of modulation in polarization sensitivity with e-vector orientation (Fig. 7B). The MWS (Fig. 7C) and LWS (Fig. 7D) cone mechanisms showed similar polarization sensitivity, with the highest sensitivity to the horizontal e-vector orientation (90 deg).

Polarization sensitivity under white light adaptation

Broad spectrum background conditions were used to examine UV polarization sensitivity. These background conditions were designed to elicit responses from both the vertical detector mechanism, mediated by the α-band of the UVS cones, and the horizontal detector

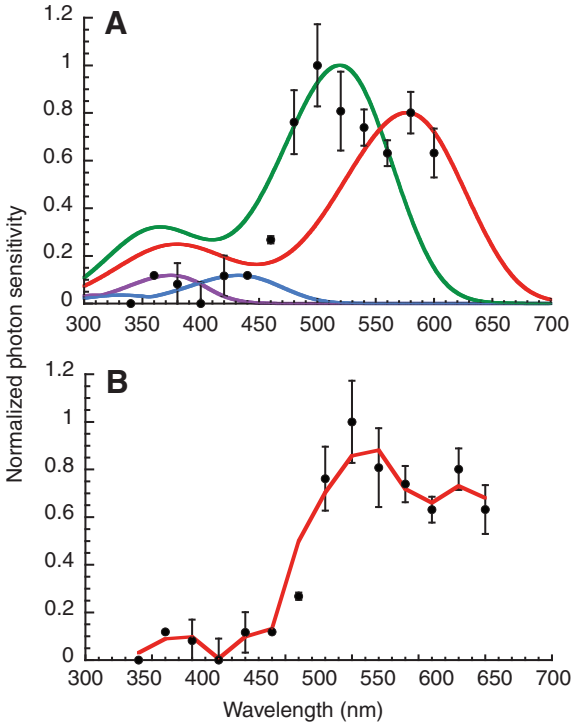

Fig. 5. Mean spectral sensitivity (±1 standard error; *N*=6) of juvenile Atlantic salmon under MWS cone mechanism isolation conditions (filled circles). (A) Least squares fit of visual pigment templates to the mean spectral sensitivity points. UVS cone (violet line), SWS cone (blue line), MWS cone (green line), LWS cone (red line) templates. (B) Least squares fit of the multiple cone mechanism model to the mean spectral sensitivity points (red line). Table 2 lists the curve fitting parameters and R^2.

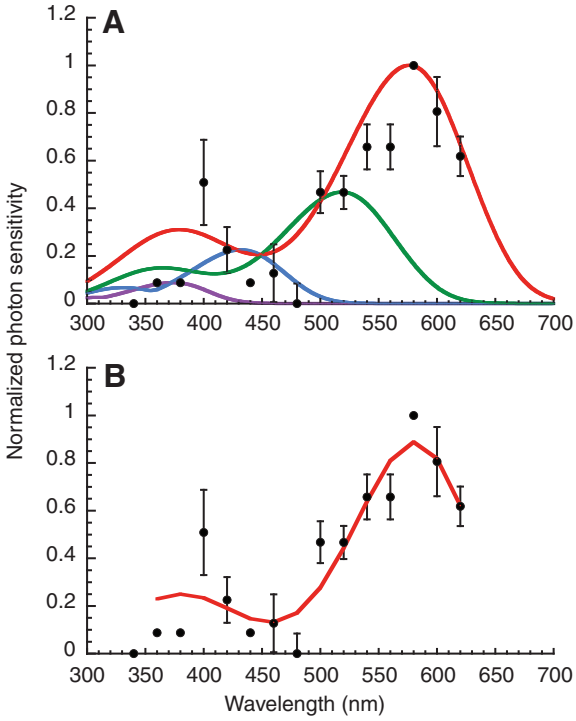

Fig. 6. Mean spectral sensitivity (±1 standard error; *N*=5) of juvenile Atlantic salmon under LWS cone mechanism isolation conditions (filled circles). (A) Least squares fit of visual pigment templates to the mean spectral sensitivity points. UVS cone (violet line), SWS cone (blue line), MWS cone (green line), LWS cone (red line) templates. (B) Least squares fit of the multiple cone mechanism model to the mean spectral sensitivity points (red line). Table 2 lists the curve fitting parameters and R^2.

mechanism, mediated by the β-band of the MWS/LWS cones. In this scenario, the polarization sensitivity curve represents a composite of both vertical and horizontal polarization detector mechanisms and these detector mechanisms interact in an opponent manner (Fig. 8A,B, Table 4). We performed both CAP and ERG recordings using UV (380 nm) linearly polarized stimuli in juvenile Atlantic salmon. When ERG recordings were used at 15 deg e-vector increments, a polarization sensitivity curve with maxima at 0 deg, 45 deg, 90 deg, 135 deg and 180 deg, and minima at 30 deg, 60 deg, 120 deg and 165 deg were found (Fig. 8A; *N*=3). The linear subtractive model was fitted to the vertical detector mechanism (open squares) and the horizontal detector mechanism (open diamonds) and Table 4 lists the curve fit parameters and R^2 values. The intermediary peaks indicated by the solid black line in Fig. 8A shows the magnitude of opponent interaction mediated by negative feedback of horizontal cells on cones (Ramsden et al., 2008). e-vector increments of 30 deg were used in conjunction with CAP recordings resulting in a polarization sensitivity curve with maxima at 0 deg, 90 deg and 180 deg, and minima at 30 deg and 150 deg (Fig. 8B; *N*=3). The linear subtractive model was fitted to the vertical detector mechanism (open squares) and the horizontal detector mechanism (open diamonds) and Table 4 lists the curve fitting parameters and R^2 values. Both the CAP (ANOVA $F_{1,6}$=0.212, P=0.662) and ERG (ANOVA $F_{1,21}$=2.152, P=0.157) polarization curves did not differ significantly from those recorded in rainbow trout (Ramsden et al., 2008).

Phylogenetic considerations of polarization sensitivity

Polarization sensitivity (PS) has been reported in *Oncorhynchus* (*O. mykiss*, *O. nerka*, *O. clarkii*), *Salvelinus* (*S. fontinalis*) (Parkyn and Hawryshyn, 2000) and *Salmo* (*S. salar*) (this study). Vertical polarization sensitivity was mediated by the UVS cone mechanism and horizontal polarization sensitivity was mediated by the MWS–LWS cone mechanisms in *Oncorhynchus* (Parkyn and Hawryshyn, 1993) and *Salmo* (this study). CAP and ERG polarization sensitivity curves were nearly identical in *Oncorhynchus mykiss* (Parkyn and Hawryshyn, 1993; Parkyn and Hawryshyn, 2000; Ramsden et al., 2008) and *Salmo salar* (Fig. 8). Polarization sensitivity is found in all the genera of the clade containing *Salmo salar*, *Oncorhynchus mykiss*, *O. nerka*, *O. clarkii* and *Salvelinus fontinalis* supporting the hypothesis that their common ancestor was UV polarization sensitive, and possessed the same mechanisms of polarization detection and processing in the peripheral visual system.

DISCUSSION

Our study describes both spectral and polarization sensitivity for the four isolated cone mechanisms of Atlantic salmon. Juvenile Atlantic salmon possess UV polarization sensitivity based on input from two differentially sensitive polarization detectors. Although little work has been conducted on the visual physiology of Atlantic salmon, the retinal morphology and development are well described (Kunz, 1987; Kunz et al., 1994). Atlantic salmon have similar retinal development to other salmonids most notably, the presence of UVS cones in the cone mosaic of juveniles and subsequent partial disappearance at smoltification and regeneration in sexually mature adults (Allison et al., 2003; Allison et al., 2006; Beaudet et al., 1993; Beaudet et al., 1997; Bowmaker and Kunz, 1987; Flamarique, 2002; Flamarique and Hawryshyn, 1996; Hawryshyn et al., 2003a).

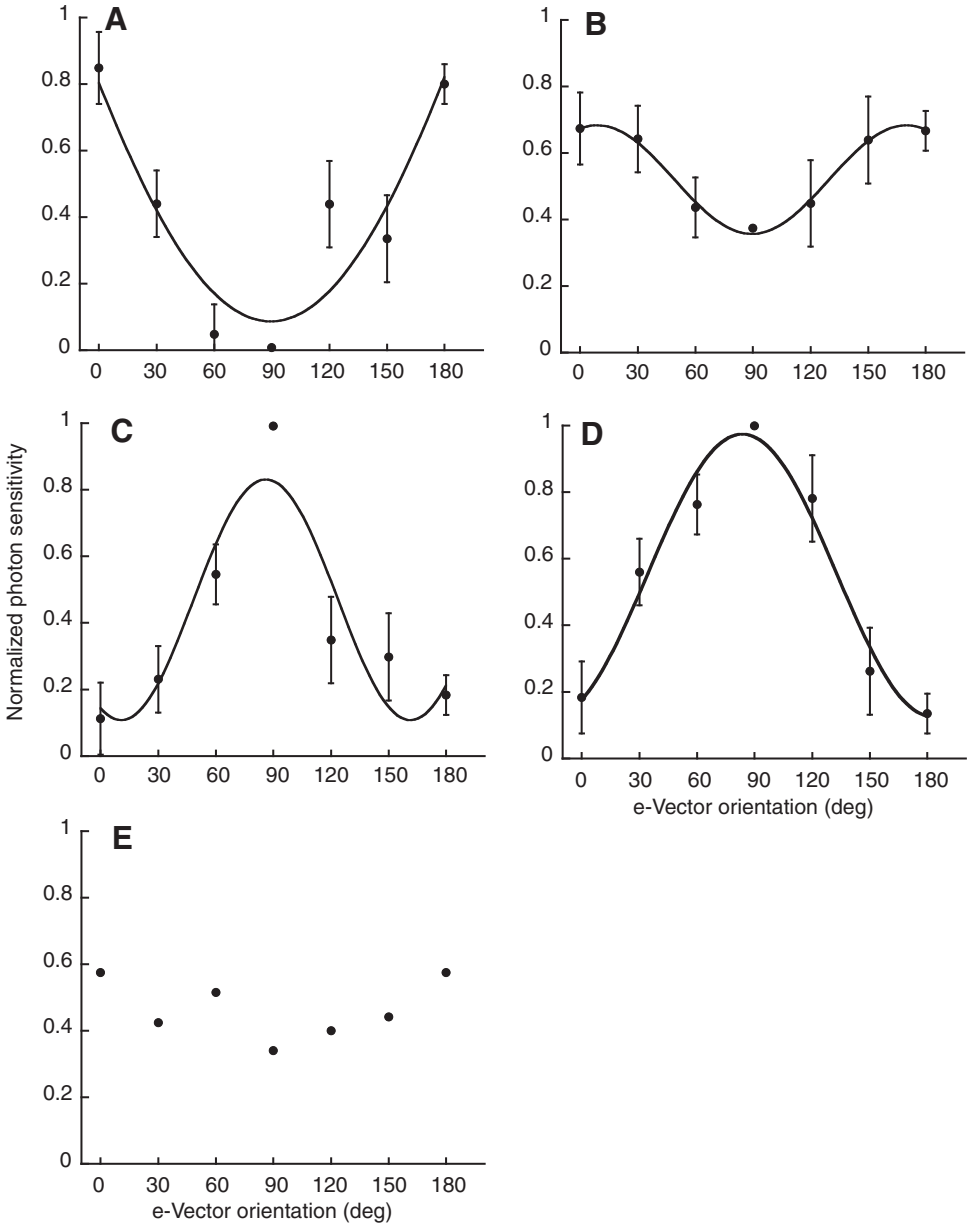

Fig. 7. Mean polarization sensitivity (±1 standard error) of Atlantic salmon for isolated cone mechanisms using chromatic adaptation. (A) Polarization sensitivity (filled circles) of isolated UVS cone mechanism (stimulus λ=380 nm; *N*=3). The line shows the least squares cosine squared function fit to mean polarization sensitivity. (B) Polarization sensitivity of isolated SWS cone mechanism (stimulus λ=440 nm; *N*=3). The line shows the least squares cosine squared function fit to mean polarization sensitivity. (C) Polarization sensitivity (circles) of isolated MWS cone mechanism (stimulus λ=540 nm; *N*=3). The line shows the least squares cosine squared function fit to mean polarization sensitivity. (D) Polarization sensitivity (circles) of isolated LWS cone mechanism (stimulus λ=660 nm; *N*=3). The line shows the least squares cosine squared function fit to mean polarization sensitivity. (E) Polarization sensitivity (circles) of isolated UVS cone mechanism light adapted by a UV background (stimulus λ=380; *N*=1). The curve fitting parameters and R^2 values are given in Table 3.

Commonality in design of polarization systems

The presence of UV polarization sensitivity in juvenile Atlantic salmon shows that this capability is broadly distributed in the Salmoninae. Our results for Atlantic salmon in comparison with previous work on Pacific salmonids show that UV polarization sensitivity is a product of the interaction between the UVS cone mechanism (α-band) – the vertical detector mechanism and MWS–LWS (β-band) cone mechanisms – the horizontal detector mechanism (Parkyn and Hawryshyn, 2000; Ramsden et al., 2008) (Fig. 7A–E). The characteristics of UV polarization sensitivity we see in the Atlantic salmon are also very similar to those described for cyprininds (Hawryshyn and McFarland, 1987), pomacentrids (Hawryshyn et al., 2003b; Mussi et al., 2005) and other salmonids (Parkyn and Hawryshyn, 2000; Ramsden et al., 2008). We argue that the conservation of UV polarization sensitivity is based on biophysical mechanisms (Flamarique et al., 1998; Roberts and Needham, 2007) within the photoreceptors that allows differential e-vector detection and the outer retina processing between photoreceptors and bipolar cells, with a significant contribution from color-opponent horizontal cells (Ramsden et al.,

Table 3. Curve fit parameters and R^2 values for polarization sensitivity of isolated cone mechanisms

Cone mechanism	e-Vector of maximum sensitivity	M_1	M_2	M_3	M_4	R^2
UVS	Vertical	0.087	2.816	0.339	59.697	0.842
SWS	None	0.520	–0.163	2.234	160.180	0.996
MWS	Horizontal	0.831	–0.773	–1.195	282.870	0.831
LWS	Horizontal	0.126	0.848	0.907	14.154	0.965
UVS adapted	None	–	–	–	–	–

M_1–M_4, curve fit parameters.

2008). Furthermore, given the remarkable similarities in UV polarization sensitivity recorded at the retinal level across several taxa, there is likely to be complementary neuronal processing at the level of the central nervous system. Our research on rainbow trout, using single unit recording in the torus semicircularis (Coughlin and Hawryshyn, 1995) describes polarization sensitive neurons that are tuned to the vertical (UV 'ON'), and horizontal (LWS 'OFF') planes of polarization.

The presence of the polarization insensitive SWS cone mechanism in Atlantic salmon points to another commonality in the design of UV polarization systems in salmonids and cyprininds. The role of the SWS cone mechanism in polarization sensitivity is not completely understood, however, the polarization insensitive SWS cone mechanism most probably monitors ambient intensity (veiling radiance), and thus sets the gain of the retinal neural network (Marc and Sperling, 1976). The overall sensitivity to the background light field is probably adjusted through the SWS cones (moderating spectral brightness differences), in a manner comparable to the polarization-insensitive long UV receptor (twisted) of honeybees (Bernard and Wehner, 1977), thus permitting the vertical and horizontal polarization detector mechanisms to operate at a higher signal-to noise ratio. Our experimental work on spatial orientation behavior in Pacific salmonids shows that the SWS cones in addition to the UVS cones must be stimulated to achieve high fidelity spatial orientation responses (Hawryshyn et al., 1990; Parkyn et al., 2003).

Phylogenetic considerations of polarization sensitivity

The similarities between the ERG and CAP polarization sensitivity curves in Atlantic salmon and rainbow trout indicate that the photoreceptor biophysical properties in addition to peripheral processing of UV polarization sensitivity is conserved between species and is based on outer retina processing between photoreceptors and bipolar cells, with a significant contribution from color-opponent horizontal cells (Ramsden et al., 2008). Both species show identical polarization sensitivity curves in the initial stages of the visual pathway (ERG). Using chromatic adaptation, the recordings at the level of the optic nerve (CAP) revealed that the cone mechanisms, forming the basis of coding ultraviolet polarized light, are identical. Furthermore, the ontogeny and organization of photoreceptors in the retinas of Atlantic salmon and other salmonids are very similar. All species of Salmoninae examined possess square mosaics with UVS cones, a fundamental requirement for UV polarization sensitivity. Thus, the evidence supports the hypothesis that UV polarization sensitivity is an ancestral character state to the species of *Oncorhynchus* (*O. mykiss*, *O. nerka*, *O. clarkii*), *Salvelinus* (*S. fontinalis*) (Parkyn and Hawryshyn, 2000) and *Salmo* (*S. salar*). To date, every salmonid species we have examined possesses the equivalent mechanisms of UV polarization vision and thus it is likely that the ancestor also possessed these mechanisms, and unlikely that the polarization neural networks evolved several times, i.e. the traits are conserved.

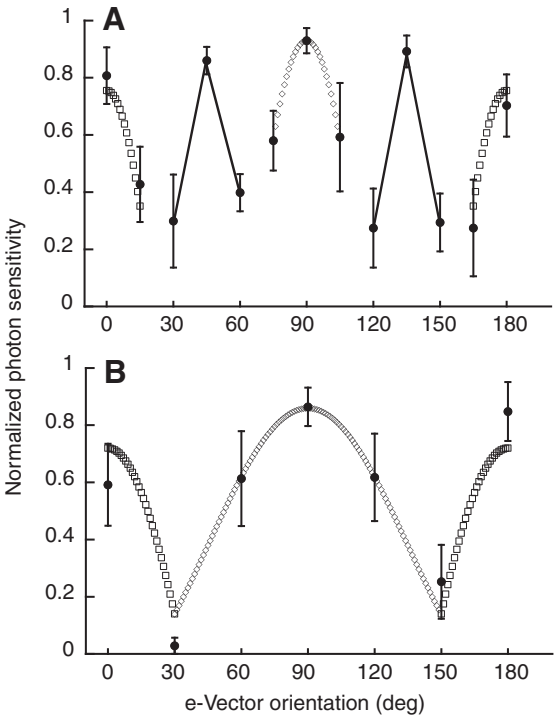

Fig. 8. Mean polarization sensitivity (±1 standard error) of Atlantic salmon using white, spectrally broad, background conditions. (A) Ultraviolet polarization sensitivity determined using ERG recording (stimulus λ=380 nm; *N*=3; filled circles). A linear subtractive model least squares fit (Table 4) to the vertical detector mechanism (open squares) and to the horizontal mechanism (open diamonds) are shown. The solid line represents the intermediary peaks showing negative feedback contribution characteristic of ERG recording in salmonids. (B) Ultraviolet polarization sensitivity determined using CAP recording (stimulus λ=380 nm; *N*=3; filled circles). A linear subtractive model fit (Table 4) to the vertical detector mechanism (open squares) and to the horizontal mechanism (open diamonds) are shown. The curve fitting parameters and R^2 values are given in Table 4.

Functional significance of UV polarization sensitivity

Our research thus far has shown that the polarization sensitivity in the UV range of the spectrum is essential for visual contrast within the complex light environments experienced by fish (Munz and McFarland, 1977). The functional linkage between UVS cones and polarization vision provides discriminative and/or contrast enhancement power that optimizes target detection and recognition capabilities. In the UV spectrum, polarization detectors interact in an opponent manner for purposes of signal conditioning. Polarization opponency functions to enhance e-vector contrast for effective coding at low degrees of polarization, and it moderates neuronal sensitivity to variations in ambient intensity, focusing activity on coding differential polarization detector input (Ramsden et al., 2008).

Our research on UV polarization discrimination in damselfish (Mussi et al., 2005) shows that the discriminative resolution can be as low as 10–15 deg difference in e-vector orientation. This subtle difference in e-vector orientation can create visual contrast that enhances both detection and recognition of targets on polarization backgrounds.

Table 4. Curve fit parameters for the linear subtractive model of UV polarization sensitivity

	V				*H*			
	e-Vector range	k_1	k_2	R^2	e-Vector range	k_3	k_4	R^2
ERG	0–15, 165–180	0.755	5.280	1.000	75–105	0.930	4.199	0.999
CAP	0–30, 150–180	0.720	1.598	1.000	30–150	0.859	0.101	0.943

k_1–k_4, curve fit parameters.
V,*H*, the response of the vertical and horizontal detector mechanisms, respectively.

We argue that UV PS serves to support several important functions including, but not limited to, plankton foraging, visual communication and spatial orientation in fishes known to have quite different life history strategies (pomacentrids, cyprinids and salmonids). It is also important to consider that a single species may have multifunctional UV polarization sensitivity effective for various modes of visual behavior. Veiling UV polarization is thought to enhance prey detection ability (Browman et al., 1994; Flamarique and Browman, 2001; Parkyn and Hawryshyn, 2000) and thus UV polarization sensitivity may enable fish to maximize capture of zooplankton and surface dwelling invertebrates. Fish have been shown to use UV reflectance patterns in intraspecific communication most notably mate choice (Macias Garcia and Burt de Perera, 2002; Rick et al., 2006; Siebeck et al., 2010; White et al., 2003), so it probable that UV PS plays an important role in enhancing these body patterns. Salmonids use UV polarization sensitivity to guide spatial orientation to polarized light fields (Hawryshyn et al., 1990; Hawryshyn and Bolger, 1990; Parkyn et al., 2003). We also know that when anadromy evolved in the Salmoninae, the ancestor had UV PS, an attribute known to guide spatial orientation. We do not claim that UV PS and anadromy are dependent on one another but we note that there is strong evidence for polarization-guided spatial orientation in salmonid fishes (Hawryshyn et al., 1990; Parkyn et al., 2003), which is important for navigation in migrating salmonids. Other taxa that possess UV PS probably share the capacity to use UV polarization in local or more global spatial orientation tasks.

Conclusions

We show that the trait of ultraviolet polarization sensitivity was present in the common ancestor to *Salmo salar*, *Oncorhynchus mykiss*, *O. nerka*, *O. clarkii* and *Salvelinus fontinalis*. The presence of UV polarization sensitivity seen across diverse taxa such as salmonids, cyprinids and pomacentrids, indicates a conservation of UV polarization sensitivity that is based on biophysical mechanisms within the photoreceptors. This allows differential e-vector detection and the outer retina processing between photoreceptors and bipolar cells, with a significant contribution from color-opponent horizontal cells. This commonality in design, especially at such early stages of vision, would suggest that UV polarization is a fundamental visual process that contributes to multifunctional visual behavior of fishes.

LIST OF ABBREVIATIONS

CAP	compound action potential recordings from the optic nerve
ERG	electroretinograms
LWS	long wavelength sensitive
MWS	mid wavelength sensitive
PS	polarization sensitivity
RI	response *versus* intensity
SWS	short wavelength sensitive
UV	ultraviolet
UVS	UV sensitive

ACKNOWLEDGEMENTS

We would like to thank the Delrymple Hatchery, British Columbia for providing fish. This research was supported by an NSERC Discovery Grant, the Canada Research Chairs program, Canada Foundation for Innovation (C.W.H.), NSERC Vanier Canada Graduate Scholarship (S.S.) and the Marguarite Adamson Estate Scholarship (S.R.).

REFERENCES

Allison, W. T., Dann, S. G., Helvik, J. V., Bradley, C., Moyer, H. D. and Hawryshyn, C. W. (2003). Ontogeny of ultraviolet-sensitive cones in the retina of rainbow trout (*Oncorhynchus mykiss*). *J. Comp. Neurol.* **461**, 294-306.

Allison, W. T., Dann, S. G., Veldhoen, K. M. and Hawryshyn, C. W. (2006). Degeneration and regeneration of ultraviolet cone photoreceptors during development in rainbow trout. *J. Comp. Neurol.* **499**, 702-715.

Beaudet, L., Browman, H. I. and Hawryshyn, C. W. (1993). Optic nerve response and retinal structure in rainbow trout of different sizes. *Vision Res.* **33**, 1739-1746.

Beaudet, L., Flamarique, I. N. and Hawryshyn, C. W. (1997). Cone photoreceptor topography in the retina of sexually mature Pacific salmonid fishes. *J. Comp. Neurol.* **383**, 49-59.

Bernard, G. D. and Wehner, R. (1977). Functional similarities between polarization vision and color vision. *Vision Res.* **17**, 1019-1028.

Bowmaker, J. K. and Kunz, Y. W. (1987). Ultraviolet receptors, tetrachromatic color-vision and retinal mosaics in the brown trout (*Salmo trutta*) – age-dependent changes. *Vision Res.* **27**, 2101-2108.

Browman, H. I., Novales Flamarique, I. and Hawryshyn, C. W. (1994). Ultraviolet photoreception contributes to prey seach behaviour in two species of zooplanktivorous fishes. *J. Exp. Biol.* **186**, 187-198.

Coughlin, D. J. and Hawryshyn, C. W. (1994). The contribution of ultraviolet and short-wavelength sensitive cone mechanisms to color vision in rainbow trout. *Brain Behav. Evol.* **43**, 219-232.

Coughlin, D. J. and Hawryshyn, C. W. (1995). A cellular basis for polarized-light vision in rainbow trout. *J. Comp. Physiol. A* **176**, 261-272.

Crespi, B. J. and Fulton, M. J. (2004). Molecular systematics of Salmonidae: combined nuclear data yields a robust phylogeny. *Mol. Phylog. Evol.* **31**, 658-679.

Flamarique, I. N. (2002). Partial re-incorporation of corner cones in the retina of the Atlantic salmon (*Salmo salar*). *Vision Res.* **42**, 2737-2745.

Flamarique, I. N. and Browman, H. I. (2001). Foraging and prey-search behaviour of small juvenile rainbow trout (*Oncorhynchus mykiss*) under polarized light. *J. Exp. Biol.* **204**, 2415-2422.

Flamarique, I. N. and Hawryshyn, C. W. (1996). Retinal development and visual sensitivity of young Pacific sockeye salmon (O*ncorhynchus nerka*). *J. Exp. Biol.* **199**, 869-882.

Flamarique, I. N. and Hawryshyn, C. W. (1998). Photoreceptor types and their relation to the spectral and polarization sensitivities of clupeid fishes. *J. Comp. Physiol. A* **182**, 793-803.

Flamarique, I. N., Hawryshyn, C. W. and Harosi, F. I. (1998). Double-cone internal reflection as a basis for polarization detection in fish. *J. Opt. Soc. Am. A* **15**, 349-358.

Govardovskii, V. I., Fyhrquist-Vanni, N., Reuter, T., Kuzmin, D. G. and Donner, K. (2000). In search of the visual pigment template. *Visual Neurosci.* **17**, 509-528.

Harosi, F. I. (1994). An analysis of two spectral properties of vertebrate visual pigments. *Vision Res.* **34**, 1359-1367.

Hawryshyn, C. W. and Bolger, A. E. (1990). Spatial orientation of trout to partially polarized light. *J. Comp. Physiol. A* **167**, 691-697.

Hawryshyn, C. W. and McFarland, W. N. (1987). Cone photoreceptor mechanisms and the detection of polarized- light in fish. *J. Comp. Physiol. A* **160**, 459-465.

Hawryshyn, C. W., Arnold, M. G., Bowering, E. and Cole, R. L. (1990). Spatial orientation of rainbow trout to plane-polarized light: the ontogeny of e-vector discrimination and spectral sensitivity characteristics. *J. Comp. Physiol. A* **166**, 565-574.

Hawryshyn, C. W., Martens, G., Allison, W. T. and Anholt, B. R. (2003a). Regeneration of ultraviolet-sensitive cones in the retinal cone mosaic of thyroxin-challenged post-juvenile rainbow trout (*Oncorhynchus mykiss*). *J. Exp. Biol.* **206**, 2665-2673.

Hawryshyn, C. W., Moyer, H. D., Allison, W. T., Haimberger, T. J. and McFarland, W. N. (2003b). Multidimensional polarization sensitivity in damselfishes. *J. Comp. Physiol. A* **189**, 213-220.

Hughes, A., Saszik, S., Bilotta, J., DeMarco, P. J. and Patterson, W. F. (1998). Cone contributions to the photopic spectral sensitivity of the zebrafish ERG. *Vis. Neurosci.* **15**, 1029-1037.

Ishiguro, N. B., Miya, M. and Nishida, M. (2003). Basal euteleostean relationships: a mitogenomic perspective on the phylogenetic reality of the "Protacanthopterygii". *Mol. Phylog. Evol.* **27**, 476-488.

Jolly, D. W., Mawdesly-Thomas, L. E. and Bucke, D. (1972). Anesthesia of fish. *Vet. Rec.* **91**, 424-426.

Kunz, Y. W. (1987). Tracts of putative ultraviolet receptors in the retina of the 2-year-old brown trout (*Salmo trutta*) and the Atlantic salmon (*Salmo salar*). *Experientia* **43**, 1202-1204.

Kunz, Y. W., Wildenburg, G., Goodrich, L. and Callaghan, E. (1994). The fate of ultraviolet receptors in the retina of the Atlantic salmon (*Salmo salar*). *Vision Res.* **34**, 1375-1383.

Li, P., Temple, S., Gao, Y., Haimberger, T. J., Hawryshyn, C. W. and Li, L. (2005). Circadian rhythms of behavioral cone sensitivity and long wavelength opsin mRNA expression: a correlation study in zebratish. *J. Exp. Biol.* **208**, 497-504.

Macias Garcia, C. and Burt de Perera, T. (2002). Ultraviolet-based female preferences in a viviparous fish. *Behav. Ecol. Sociobiol.* **52**, 1-6.

Marc, R. E. and Sperling, H. G. (1976). The chromatic organization of the goldfish cone mosaic. *Vision Res.* **16**, 1211-1224.

Munz, F. W. and Beatty, D. D. (1965). A critical analysis of visual pigments of salmon and trout. *Vision Res.* **5**, 1-17.

Munz, F. W. and McFarland, W. N. (1977). Evolutionary adaptations of fishes to the photic environment. In *Handbook of Sensory Physiology*, vol. VII (ed. F. Crescitelli), pp. 193-274. New York, USA: Springer-Verlag.

Mussi, M., Haimberger, T. J. and Hawryshyn, C. W. (2005). Behavioural discrimination of polarized light in the damselfish *Chromis viridis* (family Pomacentridae). *J. Exp. Biol.* **208**, 3037-3046.

Oakley, T. H. and Phillips, R. B. (1999). Phylogeny of salmonine fishes based on growth hormone introns: Atlantic (*Salmo*) and Pacific (*Oncorhynchus*) salmon are not sister taxa. *Mol. Phylog. Evol.* **11**, 381-393.

Parkyn, D. C. and Hawryshyn, C. W. (1993). Polarized-light sensitivity in rainbow tout (*Onchorhynchus mykiss*) – characterization from multiunit responses in the optic nerve. *J. Comp. Physiol. A* **172**, 493-500.

Parkyn, D. C. and Hawryshyn, C. W. (2000). Spectral and ultraviolet-polarisation sensitivity in juvenile salmonids: A comparative analysis using electrophysiology. *J. Exp. Biol.* **203**, 1173-1191.
Parkyn, D., Austin, J. D. and Hawryshyn, C. W. (2003). Acquisition of polarized-light orientation in salmonids under laboratory conditions. *Anim. Behav.* **65**, 893-904.
Ramsden, S. D., Brinkmann, H., Hawryshyn, C. W. and Taylor, J. S. (2003). Mitogenomics and the sister of Salmonidae. *Trends Ecol. Evol.* **18**, 607-610.
Ramsden, S. D., Anderson, L. G., Mussi, M., Kamermans, M. and Hawryshyn, C. W. (2008). Retinal processing and opponent mechanisms mediating ultraviolet polarization sensitivity in rainbow trout (*Oncorhynchus mykiss*). *J. Exp. Biol.* **211**, 1376-1385.
Rick, I. P., Modarressie, R. and Bakker, T. C. M. (2006). UV wavelengths affect female mate choice in three-spined sticklebacks. *Anim. Behav.* **71**, 307-313.
Roberts, N. W. and Needham, M. G. (2007). A mechanism of polarized light sensitivity in cone photoreceptors of the goldfish *Carassius auratus*. *Biophys. J.* **93**, 3241-3248.
Siebeck, U. E., Parker, A. N., Sprenger, D., Mathger, L. M. and Wallis, G. (2010). A species of reef fish that uses ultraviolet patterns for covert face recognition. *Curr. Biol.* **20**, 407-410.
Sperling, H. G. and Harwerth, R. S. (1971). R-G cone interactions in the increment threshold spectral sensitivity of primates. *Science* **172**, 180-184.
Temple, S. E., Ramsden, S. D., Haimberger, T. J., Veldhoen, K. M., Veldhoen, N. J., Carter, N. L., Roth, W. M. and Hawryshyn, C. W. (2008a). Effects of exogenous thyroid hormones on visual pigment composition in coho salmon (*Oncorhynchus kisutch*). *J. Exp. Biol.* **211**, 2134-2143.
Temple, S. E., Veldhoen, K. M., Phelan, J. T., Veldhoen, N. J. and Hawryshyn, C. W. (2008b). Ontogenetic changes in photoreceptor opsin gene expression in coho salmon (*Oncorhynchus kisutch*, Walbaum). *J. Exp. Biol.* **211**, 3879-3888.
Tsin, A. T. C. and Beatty, D. D. (1979). Scotopic visual pigment composition in the retinas and vitamins a in the pigment epithelium of the goldfish. *Exp. Eye Res.* **29**, 15-26.
White, E. M., Partridge, J. C. and Church, S. C. (2003). Ultraviolet dermal reflexion and mate choice in the guppy, *Poecilia reticulata*. *Anim. Behav.* **65**, 693-700.